Int. J. Electrochem. Sci., 6 **(2011)** 6483 - 6502

International Journal of
ELECTROCHEMICAL
SCIENCE
www.electrochemsci.org

Electrochemical Corrosion and Passivation Behavior of Titanium and Its Ti-6Al-4V Alloy in Low and Highly Concentrated HBr Solutions

F. El-Taib Heakal[*], *Kh.A. Awad*

Department of Chemistry, Faculty of Science, Cairo University, Giza 12613, Egypt.
[*]E-mail: fakihaheakal@yahoo.com

Received: 9 October 2011 / *Accepted:* 15 November 2011 / *Published:* 1 December 2011

Passivation and dissolution behavior of Ti and Ti-6Al-4V alloy was investigated in HBr solutions over a wide concentration range from 0.01 M to 8.0 M using open-circuit potential, electrochemical impedance spectroscopy (EIS) and potentiodynamic polarization measurements. In the low and high concentration domains, the open-circuit potential for the metal and its alloy was found to increase positively with time due to oxide film thickening on the metal surface. However, there is a certain critical HBr concentration at which the thickening rate of the oxide film on Ti metal has a maximum value. The results were confirmed by EIS measurements at open-circuit potential where a constant phase element model with its complex transfer function were used to analyze the obtained impedance responses. Polarization scans showed that the corrosion current density (i_{corr}) for titanium decreases slightly with increasing HBr concentration up to the threshold value before it starts to increase appreciably. On the other hand, for Ti-6Al-4V alloy the value of i_{corr} increases gradually with HBr concentration over the whole range, and the alloy dissolves actively due to its poor passivating ability. Interestingly, for the two materials both i_{corr} and the critical current density of passivation (i_{crit}) decrease with raising temperature, indicating a decrease in the corrosion susceptibility of the passivating oxide film as a result of the decrease in the extent of Br^- anion adsorption at higher temperatures. The apparent activation energy for the thickening process of the passive film was calculated from the increase in the spontaneous growth rate (δ_1) of its inner layer with temperature. The results in general confirmed that Ti metal has a stronger propensity to form passive film in HBr solutions better than its Ti-6Al-4V alloy.

Keywords: Titanium, Ti-6Al-4V alloy, EIS, Corrosion, Passivation

1. INTRODUCTION

Titanium and titanium-alloys are attractive metallic materials widely used as implants for dental, restorations and orthodontic wires, as well as orthopaedic due to their excellent corrosion

resistance and biocompatibility [1-4]. Titanium and its alloys present a high corrosion resistance even in very aggressive environments containing strong acidic electrolytes. This aspect is related to their inherent nature to form spontaneously dense barrier-type titanium dioxide (TiO_2), which is chemically very stable (ΔG^o_f = -889.5 kJ mol^{-1}), and increases greatly by anodic oxidation [5-8]. The good mechanical resistance/density ratio presented by Ti and its alloys make them useful candidate materials in the aerospace, aeronautic and naval industries.

In the majority of solutions and like other valve metals, Ti is in the passive state at open-circuit potential, where the thickness of its naturally formed oxide film increases linearly with time before the attainment of the steady state value [9,10]. The open circuit stability of the passive film in acidic solutions such as sulfuric, hydrochloric, phosphoric and perchloric acids has been the subject of many research papers [11-13] because of its obvious relevance to practical corrosion problems. The passive behavior of Ti in HF solution has been determined by a number of workers [14-17], and the increased film thickness was revealed to incorporate fluoride anions. Tomashov [18] reported that addition of alloying elements such as Al, V, Mo, Nb to Ti increases the steady dissolution current in the passive state, through change in the degree of defectness of passive film when the alloying atoms enter its lattice. The Ti-6Al-4V alloy with (α+β) structure has been reported to present a lower corrosion resistance than its base metal titanium in sodium azide [19] and in artificial saliva solution [20]. Most of the studies in aggressive halogen acid media were done in HCl solutions [21-24]. On the other hand, in spite of the importance of their information very few studies (if any) were directed to the corrosive hydrobromic acid solutions relevant to their influences on the corrosion characteristics of titanium and its alloys [25-27] or thin anodic oxide films on their surfaces [28]. Accordingly, it is intended in the present study to characterize the effect of concentration and ambient temperature on the electrochemical reactivity and passivation behaviour of Ti-6Al-4V alloy in comparison to its base Ti metal in hydrobromic acid solutions over low and high ranges of concentration. The techniques employed were, open-circuit potential (OCP), potentiodynamic polarization and electrochemical impedance spectroscopy (EIS). An equivalent electronic circuit model for the electrochemical system was suggested and the impedance data were obtained by fitting the experimental data to an appropriate proposed circuit model.

2. EXPERIMENTAL

The working electrodes were made from spectroscopically pure titanium and Ti-6Al-4V alloy with composition in wt.% of: 5.70 Al, 3.85 V 0.18 Fe, 0.038 C, 0.106 O, 0.035 N. The two electrodes were supplied in the form of massive cylindrical rods from Johnson and Malthey (England). Each metallic rod was welded to an electrical wire and fixed with epoxy resin in a glass jacket, leaving a fixed exposed surface area of 0.196 and 0.384 cm^2 for titanium and titanium alloy, respectively throughout the whole measurements. The electrode surfaces were mechanically abraded using finer grades of emery papers (600-1200 grit) followed by 0.2 μm diamond past polishing to give a mirror-like finish. All potentials were measured and reported with reference to a saturated Ag/AgCl/KCl electrode. Test solutions ranging from 0.01 M up to 8.0 M were prepared from AnalaR grade

concentrated hydrobromic acid solution (BDH) by appropriate dilution using ultra pure water (~47 wt.% being the azeotropic composition of HBr solution)**.** Open-circuit potential (OCP), polarization and electrochemical impedance spectroscopy (EIS) measurements were performed using the electrochemical workstation IM6e impedance analyzer (Zahner-electrik GmbH, Meβtechnik, Kronach, Germany) provided with Thales software. The excitation signal was a 10 mV sinusoidal potential through a frequency domain from 100 kHz down to 100 mHz [19]. The impedance diagrams were recorded at the steady OCP, while polarization scans were traced at a rate of 1 mV s^{-1} starting from -0.5 to 1.0 V vs. Ag/AgCl. The experiments were always carried out inside an air thermostate, which was kept at 25^{o}C, unless otherwise stated. Each experiment was repeated at least three replicates using freshly prepared solution in every time and the average of the most reliable data was taken.

3. RESULTS AND DISCUSSION

3.1 Effect of hydrobromic acid concentration

3.1.1 Open circuit behavior

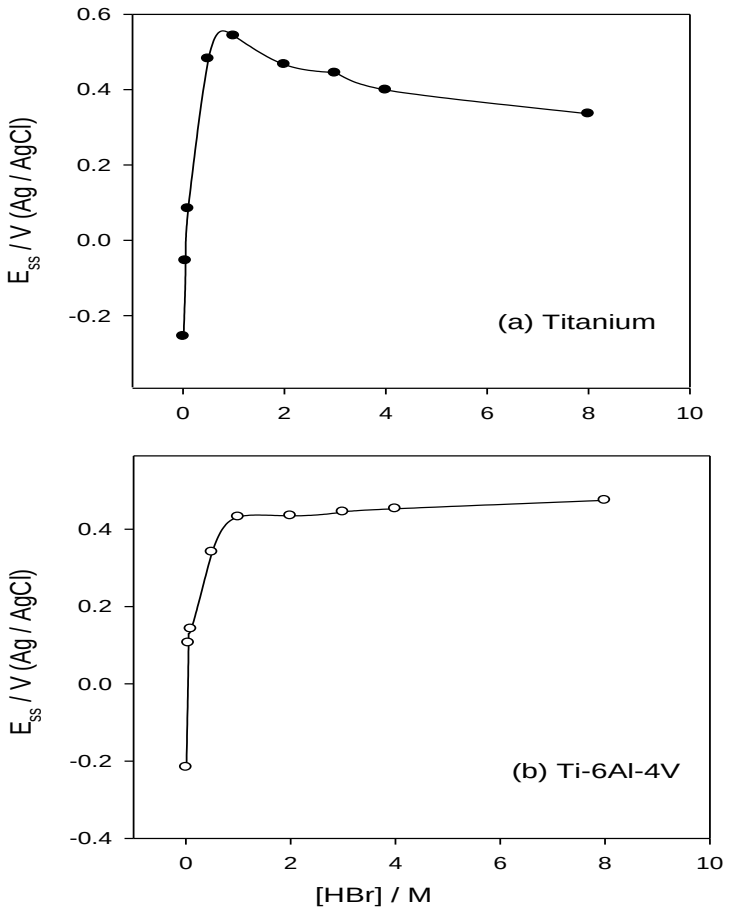

Figure 1. The steady-state OCP (E_{ss}) as a function of HBr molar concentration for: (a) titanium and (b) Ti-6Al-4V alloy at 298 K.

Over a wide concentration range (0.01 - 8.0 M) from HBr solutions, all OCP transients for both Ti and Ti-6Al-4V alloy are found quite similar in nature, where the potential of each sample drifts in the noble direction immediately after immersion and gradually approaches a quasi-steady state value (E_{ss}) within 20 min. In the tested naturally oxygenated HBr electrolyte, the positive shift of potential indicates spontaneous passivation by healing and further thickening of the pre-existing native oxide film on the metal surface [19,29,30]. Fig. 1a, b shows the dependence of the steady potential for Ti and its alloy on HBr concentration. As can be seen, for each metallic material E_{ss} reveals an abrupt increase in the positive direction of potential with increasing HBr concentration up to ~1.0 M, whereby it becomes concentration independent for Ti-6Al-4V alloy.

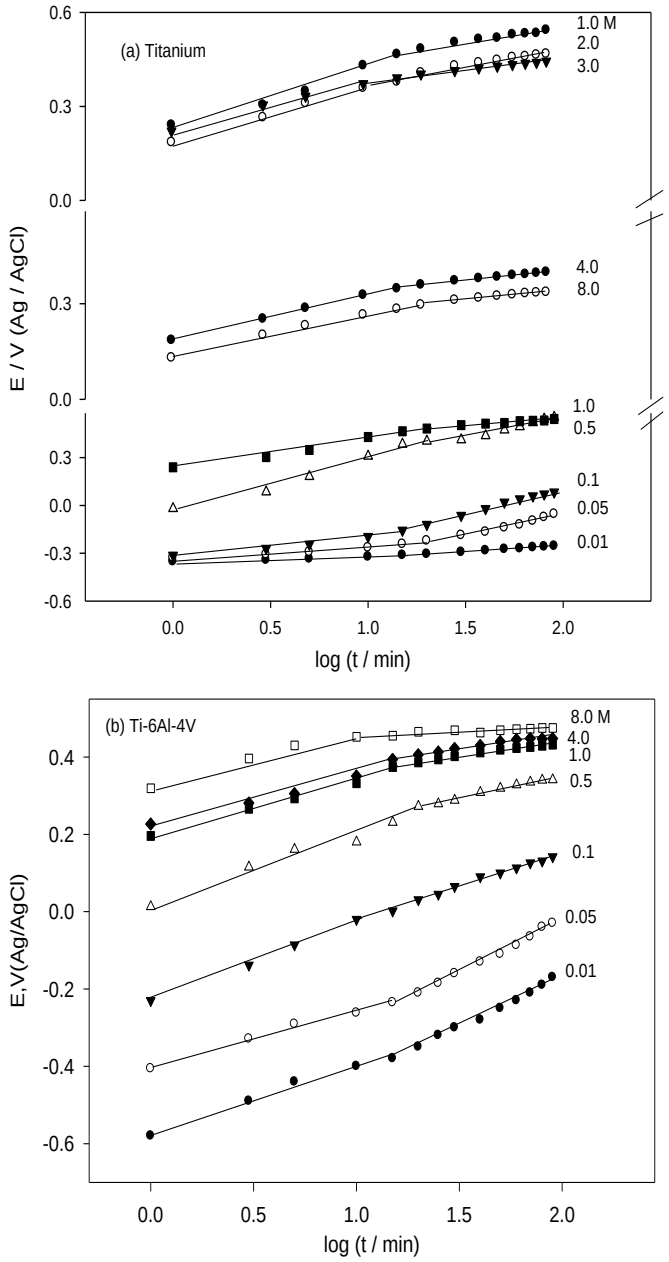

Figure 2. *E*-log*t* plots for: (a) titanium and (b) Ti-6Al-4V alloy in HBr solutions of different concentrations at 298 K.

While for titanium E_{ss} resumes a small decrease before attaining a quasi-steady value. Such behavior is likely attributed to competitive adsorption of aggressive Br^- ion with oxygen on the oxide surface. Thus, in aerated dilute HBr solutions (≤1.0 M), oxygen has higher affinity than Br^- ion for adsorption on the surface, the adsorbed oxygen causes thickening of the oxide film as inferred from the sharp positive increase of E_{ss} from -0.3 to more than +0.4 V vs. Ag/AgCl. However, in concentrated HBr solutions (>1.0 M), the adsorbed Br^- ions on the oxide surface succeed to destroy surface passivity by displacing adsorbed oxygen and partially dissolving the oxide film. Thereby, E_{ss} decreases to some extent until it reaches a limiting value at which the two rates for oxide formation and dissolution processes become equal.

Under open circuit conditions, it was suggested that the driving force for surface oxide film formation on the metal is the free energy change of the reaction between the metal and the test solution. This process is assumed to proceed via solid state mechanism by the influence of a sufficiently high electric field to cause ionic migration and hence sustain self-diffusion of metal ions through semiconducting oxide films [31]. Based on this notion a relationship between E and log t has been theorized [9] as given by the following equation:

$$E = constant + 2.303\,(\delta/B)\log t \qquad (1)$$

where δ is the rate of oxide film thickening per decade of time and B is a constant [9,19]. Fig. 2a, b shows the applicability of this equation to the present results for Ti and its alloy. Each plot in the figure consists of two straight line segments corroborating that the formed passive film is of a duplex nature in accordance with the point defect model (PDM) by Macdonald [32].

Table 1. Thickening rates δ_1 and δ_2 (in nm / decade) for the inner and the outer layers of the spontaneous passive films on Ti and Ti- 6Al-4Valloy surfaces as a function of HBr concentrations.

Electrode	[HBr] / M	δ_1 / nm decade^{-1}	δ_2 / nm decade^{-1}
Ti	0.01	0.60	1.37
	0.05	1.36	4.76
	0.10	2.22	5.01
	0.50	5.92	5.23
	1.0	3.33	1.44
	2.0	2.84	1.38
	3.0	2.44	1.05
	4.0	2.35	0.95
	8.0	2.20	0.90
Ti-6Al-4V	0.01	3.30	3.63
	0.05	3.44	4.27
	0.10	3.56	4.41
	0.50	3.84	4.45
	1.0	2.49	1.17
	4.0	2.10	0.91
	8.0	2.00	0.40

The first segment is attributed to the formation of a very thin barrier type oxide layer, whereas the second is related to longer immersion times, indicating formation of a thicker outer film. The rates of thickening for both forms of oxide, δ_1 (for the inner) and δ_2 (for the outer) were computed from the slopes of these plots as given in Table1.

The results show that at high HBr concentrations (>0.5 M) the rate of oxide growth for each sample decreases gradually with concentration. However, at low range of concentration both δ_1 and δ_2 for Ti showed a sudden increase in their values up to 0.5 M, while for Ti-6Al-4V alloy the increase is not appreciable.

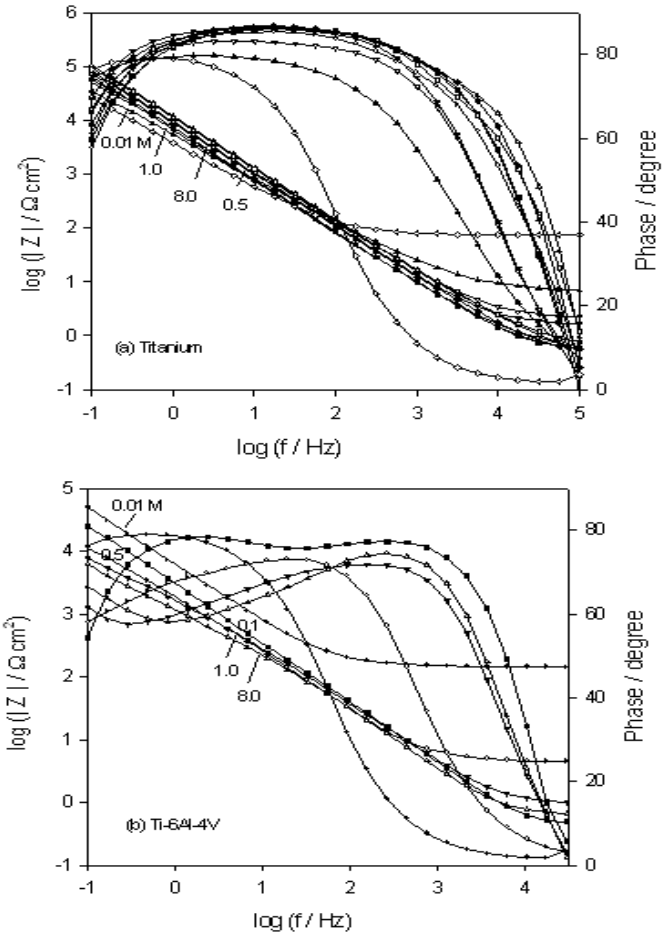

Figure 3. Bode plots for: (a) titanium and (b) Ti-6Al-4V alloy in HBr solutions of different concentrations at 298 K.

This behavior suggests that hydrobromic acid medium favors self-passivation of titanium and Ti-6Al-4V alloy, where the highest efficacy towards passive film formation was observed in 0.5 M solution. This is explicable in terms of an enhancement in the rate of oxide dissolution than the rate of its formation as the acid concentration is increased more than 0.5 M. On the other hand, the results clearly indicate that although addition of aluminum and vanadium as alloying elements to titanium

improves its mechanical traits, it increases the susceptibility of passive layers on the metallic surface to chemical dissolution in HBr medium, The dissolution may be due to the presence of additional oxides [2,33], which enter the lattice of the passive film rendering it more defective, and hence the film becomes less stable. This can be readily seen from the lower δ_1 and δ_2 values for the alloy in comparison to those for pure titanium metal at higher HBr concentrations (>0.1 M).

Results of EIS seem to offer further confirmation for the extent of surface reactivity of Ti and Ti-6Al-4V alloy under open circuit conditions in HBr media. The low frequency capability has led EIS to probe and readily detect relaxation phenomena involving surface intermediates and thus studying electrochemical corrosion and passivation mechanisms. Prior to the impedance scan each specimen was left immersed in the test solution until a steady state OCP was reached. All measurements were carried out in the frequency domain 100 kHz -100 mHz, and the data are presented as Bode plots for both electrodes in Fig. 3(a, b) as a function of HBr concentration over the range 0.01 M - 8.0 M. Bode plot is recommended as a standard impedance plot, since all impedance data are equally represented and the phase angle is a sensitive index to the surface phenomena occurring at the electrode/electrolyte interface [34-36]. As can be seen, the spectra in Fig. 3 reveal highly capacitive response typical of passive materials, as indicated by the phase angle remaining close to 90^o over a wide range from medium to low frequencies. This behavior is more accentuated for titanium and suggesting the formation of more stable film on the pure metal as compared to its Ti-6Al-4V alloy. For both samples it can be noted that, although the electrochemical impedance was measured down to a low frequency of 100 mHz, no horizontal impedance plateau can be discerned in the spectra over this frequency range, while in the high frequency region log $|z|$-log f relation tends to become constant with a phase angle drops towards zero degree [4,19]. This is a typical resistive behavior corresponding to the solution resistance between the working and reference electrodes.

Moreover, the large broad phase angle peak indicates an interaction of two time constants, reflecting the bi-layer nature of the passive film on Ti and its alloys comprising a porous outer layer and a barrier inner layer [19,37]. Based on these facts the obtained EIS data were analyzed in terms of the equivalent circuit (EC) shown in Fig. 3c, which was proposed to simulate the metal/oxide/solution interface for Ti and its alloy [19]. The EC model consists from a simple Randles circuit representing the charge transfer resistance and double layer capacitance (R_{ct} and C_{dl}) branched in parallel arrangement with the resistance and capacitance of the passivating oxide film (R_{ox} and C_{ox}), and the whole are series connected with the solution resistance(R_s) [19]. A non-ideal capacitive response of the oxide film was taken into account by using a constant phase element (CPE) instead of a pure capacitance in the fitting procedure. This CPE can be related to a distribution of relaxation times as a result of different degrees of surface in-homogeneity, roughness effects and variations in properties or compositions of surface layers [38]. The impedance associated with the capacitance of the oxide layer is described by the complex frequency dependent impedance (Z_{CPE}) defined as [19,35, 38- 40]:

$$Z_{CPE} = 1/Q_o(j\omega)^x \qquad (2)$$

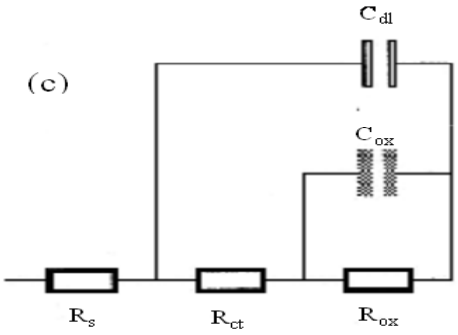

Figure 3c. Electrical equivalent circuit used to analyze the present experimental EIS data.

Table 2. Equivalent circuit parameters for the spontaneously formed passive film on (a) titanium and (b) Ti-6Al-4V alloy as a function of HBr concentration at 298 K.

[HBr] / M	R_{ox} / kΩ cm^2	C_{ox} / μF cm^{-2}	x	R_{ct} / Ω□ cm^2	C_{dl} / μF cm^{-2}	R_s / Ω
(a) Titanium						
0.01	220.7	20.99	0.89	9.90	8.72	367.3
0.10	235.4	10.01	0.86	13.85	7.98	34.0
0.50	309.2	4.26	0.87	7.29	6.65	11.39
1.0	292.7	4.39	0.89	18.57	6.54	8.95
2.0	267.2	4.45	0.85	10.24	8.75	3.94
3.0	239.4	4.60	0.95	15.63	9.01	3.47
4.0	180.7	4.84	0.89	0.23	9.43	2.93
5.0	180.1	5.61	0.94	17.20	9.92	3.13
6.0	140.1	6.13	0.95	18.72	11.03	3.37
8.0	110.9	6.86	0.99	7.74	13.22	3.59
(b) Ti-6Al-4V						
0.01	165.1	2.20	0.90	24.12	2.87	365.60
0.10	146.2	2.31	0.85	22.10	8.85	11.98
0.50	123.3	2.68	0.84	19.29	12.13	2.83
1.0	97.4	3.29	0.85	15.13	13.48	1.83
4.0	86.2	3.32	0.75	12.20	14.32	1.65
8.0	77.5	3.46	0.81	9.83	15.13	1.39

where Q_o is the magnitude (Ω^{-1} cm^{-2} s $^{-x}$) of the CPE which is identical to the idealized capacitance (C_{ox}) at ω =1, ω being the angular frequency ($\omega = 2\pi f$ rad s^{-1}), and $j = (-1)^{1/2}$. The value of x can vary between 1 for a perfect capacitor and -1 for a perfect inductor. Fitting procedures using the following (Eq. 3) transfer function [41] for the proposed EC model (Fig. 3c) adequately described the measured data to an error of 5% or less, and the calculated EC parameters are listed in Table 2.

$$Z_{EC} = R_s + \cfrac{1}{j\omega c_{dl} + \cfrac{1}{R_{ct} + \cfrac{1}{(j\omega c_{ox})^x + \cfrac{1}{R_{ox}}}}} \quad (3)$$

The results indicate that although the parameters are all concentration dependent, the values of R_{ox} are greater than those for R_{ct}, by more than 1.5×10^4 times, which assumes the presence of a protective oxide film providing a high corrosion resistance to the sample. Therefore, the influence of the double layer on the total impedance of the interface seems to be comparatively negligible, and accordingly the EIS data become dominated by the passive film properties.

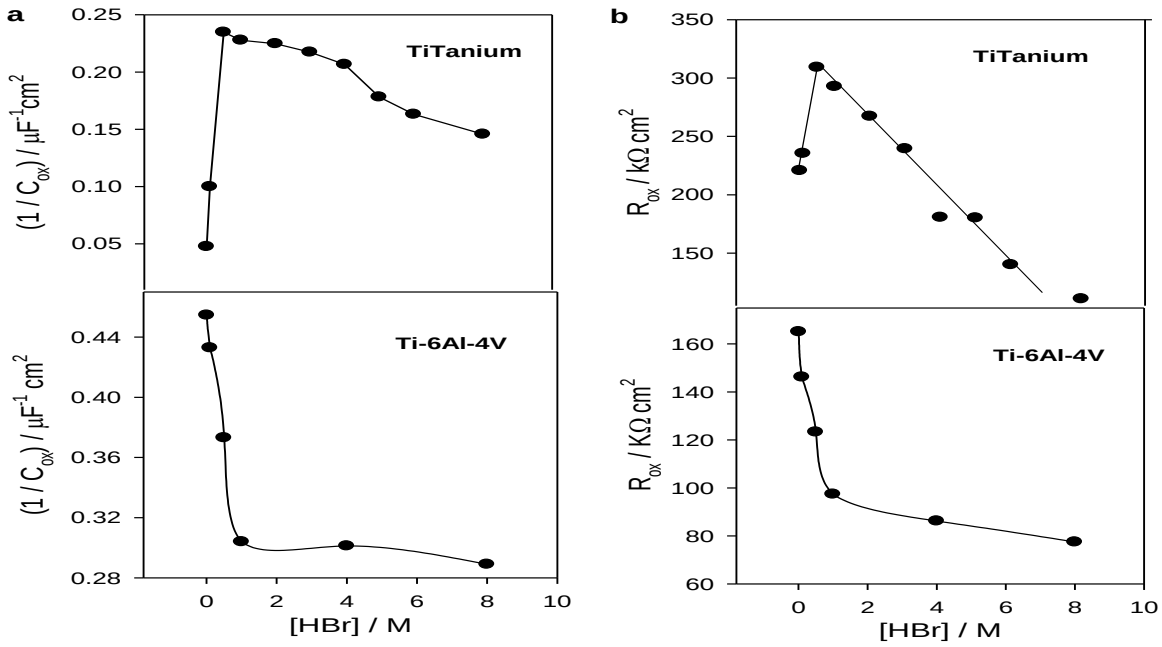

Figure 4. Dependence of: (a) the relative oxide film thickness ($1/C_{ox}$) and (b) its resistance (R_{ox}) on HBr molar concentration at 298 K.

Variation of the values of ($1/C_{ox}$), which is directly proportional to the relative thickness of the oxide film [19,28,39,40], as well as its resistive component (R_{ox}) with HBr molar concentration are depicted in Fig. 4(a, b) for titanium and Ti-6Al-4V alloy, respectively. For each sample, it is observed that the behavior of the two parameters follows an almost similar pattern. Thus, for titanium metal there is an initial linear fast increase in the values of the relative film thickness and its resistance with increase in HBr concentration up to 0.5 M followed by a gradual decrease in their values at higher

concentrations (>0.5 M HBr). However, in the case of Ti-6Al-4V alloy the general trend for the variation of those two parameters is an exponential decrease over the whole concentration range (0.01 M - 8.0 M) with no sign for a critical concentration. Thereby, for both samples the EIS behavior is commensurate with that for OCP results and suggesting that HBr can promote spontaneous growth of passivity oxide films on Ti and Ti-6Al-4V surfaces. Those passive films inhibit active dissolution of the underlying metal and protect it from corrosion. Nevertheless, the issue of the resistance to active anodic dissolution and propensity for passivation appears to be a function of the forming HBr concentration and the metallic substrate composition. Various factors may be involved to bring about such results.

In reducing bromide acid medium the presence of a native TiO_2 film on the sample surface is a formidable barrier to localized corrosion. However, the present results indicate that TiO_2 can fail and leads to localized corrosion, including pitting attack, in the presence of aggressive Br^- anion [40, 42]. A possible mechanism for TiO_2 failure may be through pit nucleation [27]. In bromide media over the low concentration range (0.01 M - 0.5 M), it can be assumed that a surface defect in the metal favors an increase in localized growth of the passive film. This defect appears as an area for a pit nucleus at which a selective halide ion mass transfer may occur and favoring the formation of titanium tetrahalide (or oxyhalide) [43] via the reaction

$$Ti + 4Br^- = TiBr_4 + 4e \quad (4)$$

to take place that can be serve as a substitution for the reaction

$$Ti + 2H_2O = TiO_2 + 4H^+ + 4e \quad (5)$$

which accounts for the passivity of titanium surfaces.

As passivity and pitting are dynamic processes, water molecule diffusion leads to hydrolyse the salt at the boundary between the $TiBr_4$ clusters and the solution and regenerate Br^- ion via the reactions

$$TiBr_4 + 2H_2O = TiO_2 + 4Br^- + 4H^+ \quad (6)$$

and/or

$$TiBr_4 + H_2O = TiO^{++} + 4Br^- + 2H^+ \quad (7)$$

The oxide (TiO_2) and/or the titanyl ion (TiO^{++}) repassivate the surface and should decrease or even stop the dissolution at the micro-pits, as long as Br^- ion concentration is low ($\leq$ 0.5 M) and the electric field is not high enough to secure, by ionic conduction, the mass transport across the phase boundary. However, at higher Br^- ion concentrations (> 0.5 M), local aggressive conditions are established and an increase in the mass transfer occurs with a subsequent breakdown in the dynamic

equilibrium between passivation and dissolution within the pits, leading to a decrease in the passive film resistance (R_{ox}) and a concomitant diminution in the film thickness ($1/C_{ox}$) value.

3.1.2 Potentiodynamic polarization behavior

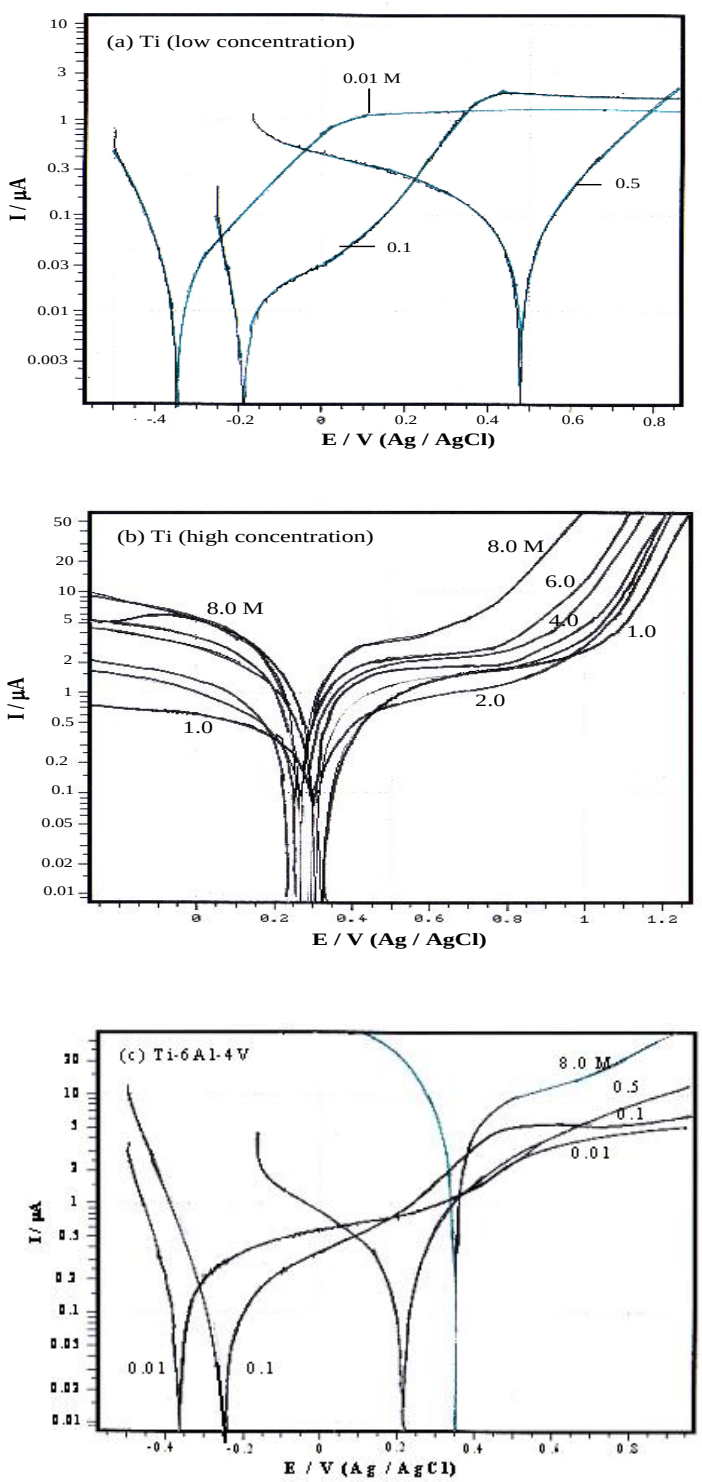

Figure 5. Potentiodynamic cathodic and anodic polarization scans for: (a,b) titanium, and (c) Ti-6Al-4V alloy as a function of HBr molar concentration at 298 K.

Cathodic and anodic linear sweep curves for Ti and Ti-6Al-4V recorded at a scan rate of 1 mV s^{-1} are presented in Fig. 5(a-c) in relation to HBr concentration in the domain of 0.01 M to 8.0 M. As the results reveal, the polarization scans exhibit Tafel behavior.

At all acid concentrations the cathodic curves are quite similar for the metal and its alloy, indicating similar cathodic reaction takes place on both materials. When the anodic polarization starts, the current in the active region increases rapidly due to metal ion dissolution. As the potential increases in the positive direction the rate of variation of the anodic current decreases and the curve merges into a more or less plateau very dependent on the electrolyte concentration before possible evolution of O_2 and /or Br_2 takes place on the passive electrode surface, characterized by a re-increase in the polarizing current.

Table 3. Electrochemical corrosion parameters of Ti and Ti-6Al-4V alloy as a function of HBr concentration at 298 K.

[HBr] /	E_{corr} /	i_{corr} /	η_c /	η_a /	i_{crit} /	E_{crit} /
M	$mV_{Ag/AgCl}$	μA cm^{-2}	mV / decade	mV / decade	μA cm^{-2}	mV
(a) Titanium						
0.01	-335	0.10	-11	190	5.15	28.88
0.1	-180	0.05	-111	125	4.42	121.0
0.5	480	0.03	-185	141	4.81	672.0
1.0	320	0.36	-413	211	5.70	448.7
2.0	290	0.90	-283	276	3.64	483.0
3.0	230	1.51	-266	239	5.02	353.0
4.0	310	1.82	-251	260	5.15	450.0
5.0	300	2.96	-206	294	7.83	451.5
6.0	260	3.91	-304	405	10.50	449.1
8.0	250	4.70	-256	318	11.20	450.0
(b) Ti-6Al-4V						
0.01	-360	0.19	-72.0	145.0	0.65	-270
0.1	-250	0.22	-121	361.0	0.56	-117
0.5	210	1.10	-206	119.0	2.04	-267
1.0	260	1.38	-97.5	91.90	9.70	275
8.0	350	8.28	-41.3	24.30	24.01	514

The electrochemical dissolution parameters for titanium and its alloy were estimated using Thales software for i/E analysis [19,44] and listed in Table 3. The results indicate clearly that all these parameters are strongly dependent on both solution composition and electrode material. The corrosion current density (i_{corr}), which is equivalent to the corrosion rate, was determined by intersection of the cathodic Tafel line with the corrosion potential (E_{corr}) value of zero current. It has to be noted that E_{corr} determined from polarization curves are significantly lower than those obtained from the OCP measurements. This is expected, as the polarization tests were started at a cathodic potential relative to

the corrosion potential, so that the passive film at the surface was at least partially removed due to the highly reducing initial potential [4,45]. Figure 6(a, b) displays the dependence of log i_{corr} on log HBr molar concentration. For titanium, the figure illustrates that i_{corr} decreases slightly with increasing concentration up to 0.5 M before it resumes to increase appreciably. The recorded increase in i_{corr} at higher concentrations (> 0.5 M) may be ascribed to a decrease in the efficiency of oxide building caused by the aggressive influence of Br^- ions.

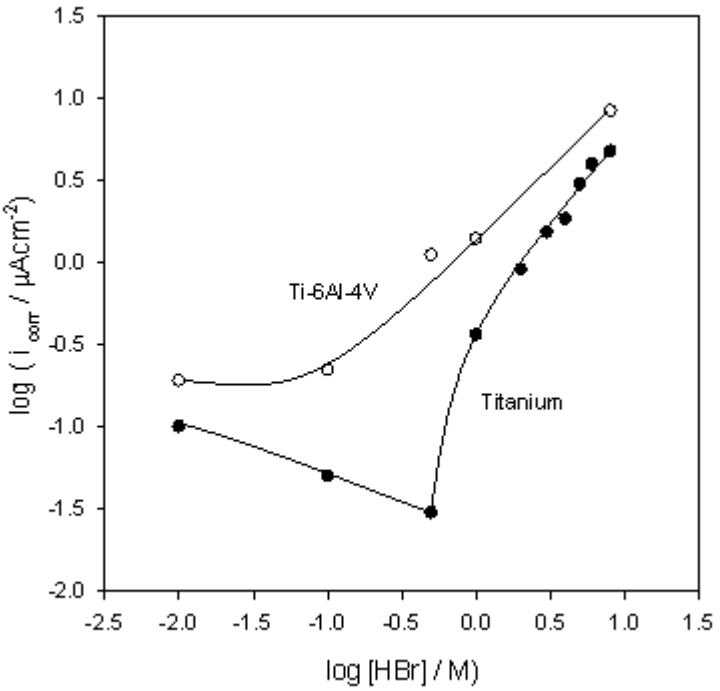

Figure 6. Dependence of i_{corr} on HBr molar concentration for (a) titanium and (b) Ti-6Al-4V alloy.

So, it is possible to assume that Br^- as depassivating anions play their activating role through preferential adsorption on the oxide surface and hence can participate in enhancing the formation of soluble complexes, most likely clusters of $TiBr_4$ molecules [27]. These compounds initiate pits nucleation at the active inclusion sites on the electrode surface, leading to partial inhibition in the oxide growth process associated with an increase in the corrosion rate (i_{corr} value). However, in more diluted solutions ($\leq$ 0.5 M), the depassivating action of Br^- anions becomes less important compared to the high efficiency of the metal to oxygen [46] and thus i_{corr} value decreases.

On the other hand, in case of Ti-6Al-4V alloy, the value of i_{corr} increases gradually with concentration over the whole range (0.01-8.0 M), and the alloy dissolves actively as the Br^- ion concentration in the medium increases (cf. Fig. 6(b)). The enhanced corrosion of the alloy, especially over the lower HBr concentrations, as compared to the corrosion behavior of the pure metal can be attributed to the presence of more point defects in the structure of the passive layers of the alloy caused by the strong influence of the alloying elements in Ti-6Al-4V [47]. The higher defect concentration in the oxide film increases the penetration of the aggressive Br^- anions, thereby decreases its resistance to corrosion and leading to i_{corr} increase. It has to be noted that pitting of passivated Ti surface is limited

to high anodic overpotential (> 5 V vs. OCP) even in aggressive halide containing solutions. For example, in 1.0 M NaBr at 30 ^{o}C environment, Shibata and Zhu [48] have reported a value of +6.0 V (vs SCE) for the titanium pitting potential. Inspection of Table 3 reveals also that the critical current density (i_{crit}) for both samples behaves in a similar manner as i_{corr} with respect to the influence of HBr concentration, where these two parameters are always inferior for titanium than for its alloy at any given Br^- ion concentration. The results indicate that Al and V addition to titanium as alloying elements has a detrimental effect concerning its corrosion vulnerability in HBr medium. In addition, the data indicate that E_{crit} exhibits a comparable trend to that of E_{corr} for each material, which is in good agreement with the OCP behavior.

3.2 Effect of Temperature

The influence of temperature on the stability of spontaneously formed passive films on Ti and Ti-6Al-4V alloy was studied in HBr medium. Previously, Blackwood and Peter [49] found that high defect densities associated with rapidly grown oxide films on Ti in H_2SO_4 could be decreased by growing or annealing the oxide films at higher temperatures. Also, Shibata and Zhu [50] reported that the dielectric constant for the anodic film on Ti in H_2SO_4 solution increases with temperature.

3.2.2 Open circuit behavior

The effect of temperature on the time profile of the OCP behavior of freshly polished Ti and Ti-6Al-4V electrodes was investigated in naturally aerated 1.0 M HBr solution over the range 280 - 318 K. The OCP of the alloy was found to be always more negative than that for the metal. Nevertheless, in both cases the OCP became nobler with increasing immersion time until reached the steady-state value (E_{ss}). For each electrode, the measured E_{ss} increases exponentially with rise in temperature. It seems that a very stable surface layer was formed as soon as the sample was contacted HBr solution. The results imply that moderate acid concentration (1.0 M) promotes additional passivation for both samples at higher temperatures. Such behavior indicates that increasing temperature of HBr solution favors oxide film formation and growth on the expense of oxide film dissolution process. Hence in bromide medium, temperature can act as a catalyst for easier movement of the cations and anions which would lead to evolution of oxide layers at the oxide/solution interface and also presumably repairing the flawed regions on the sample surface [30].

Basically, the OCP transients are able to yield information on the rate of spontaneous metal passivation [19,36]. Thus, by considering the OCP variation with log t as a function of temperature for Ti and its alloy, linear plots are obtained following Equation (1), where the slope (δ) of each plot is directly proportional to the rate of oxide growth. Indeed, each plot consists of two intersecting linear segments, which reflects the duplex nature of the growing oxide film. Fig. 7 shows the effect of temperature on the oxide formation efficiency (of its inner layer) in 1.0 M HBr solution under open circuit conditions for the two tested samples. The plots of log δ_1 versus $1/T$ are linear following the familiar Arrhenius equation. Values of the apparent activation energy (E_a) calculated from the slopes

of the two plots are 6.19 and 8.10 kJ mol^{-1} for Ti and Ti-6Al-4V alloy, respectively. These results indicate that although Al and V addition to titanium does not, in principle, modify the protection characteristics of its spontaneous oxides, pure Ti exhibits a stronger propensity to enhance the growth rate of the passivating oxide layers than its alloy, with increasing ambient temperature.

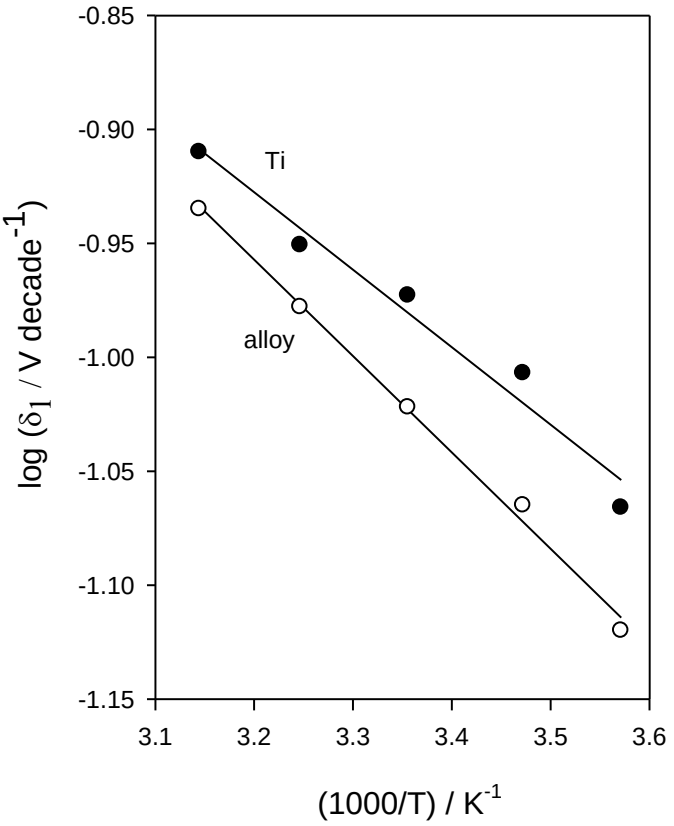

Figure 7. Thickening rate of the inner layer (δ_1) as a function of temperature in 1.0 M HBr solution for titanium and Ti-6Al-4V alloy.

For additional information concerning the role of temperature on the corrosion vulnerability and passive behavior of the oxide layers on Ti and its alloy, EIS Bode plots of the two samples were probed at the rest potential (E_{ss}) after 100 min immersion in 1.0 M HBr solution as a function of temperature.

The fitting procedures using the same equivalent circuit model shown in Fig. 3c were found to give better agreement between the theoretical and experimental data. Table 4 presents the derived impedance parameters for the two samples. Fig. 8 reveals that oxide film resistance (R_{ox}), which determines the insulating property of the oxide layers, increases linearly for both samples as the temperature increases with a concomitant increase in the relative thickness ($1/C_{ox}$) of their passive films. Furthermore, at any identical experimental conditions, R_{ox} for Ti is always much higher than that for the alloy, in spite that $1/C_{ox}$ for the former is lower.

Table 4. Equivalent circuit parameters of Ti and Ti-6Al-4V alloy in 1.0 M HBr solution at different temperatures.

Electrode	T / K	R_{ox}	C_{ox}	x	R_{ct}	C_{dl}	R_s
		kΩ□ cm^2	μF cm^{-2}		Ω cm^2	μF cm^{-2}	Ω
Ti	280	269.1	4.62	0.86	17.91	6.65	9.45
	288	283.3	4.45	0.85	17.80	6.61	9.52
	298	292.7	4.39	0.89	18.57	6.54	8.95
	308	307.1	4.15	0.83	20.65	6.14	10.10
	318	316.2	4.06	8.87	19.21	6.32	9.72
Ti-6Al-4V	280	76.1	3.66	0.85	11.50	15.20	1.85
	288	83.2	3.51	0.84	13.01	16.10	1.90
	298	97.4	3.29	0.85	15.13	13.48	1.83
	308	107.3	3.01	0.86	18.20	13.01	1.40
	318	114.2	2.85	0.85	21.30	13.50	1.89

Such behavior indicates formation of a thinner, more compact and dense oxide film on pure Ti as compared to the thicker oxide layer with a defective nature and more open structure grown on Ti-6Al-4V alloy surface. Thereby, thin oxide films which formed on the pure metal are more protective than the thicker ones formed on its alloy as being with lower resistance.

3.2.2 Polarization behavior

Polarization scans (not seen) as a function of temperature for the present tested samples were collected after a holding time of 100 min. in naturally aerated 1.0 M HBr solution. A fresh solution was used for each experiment at the required temperature within the range 280-318 K. Upon raising solution temperature no significant differences in the polarization characteristics are observed, except a continuous general shift of the whole Tafel plot towards more positive potential values and a decrease in the polarizing current. This is typical of a passive behavior. The electrochemical corrosion parameters were evaluated from the polarization curves and presented in Table 5. The results indicate clearly that all parameters are dependent on the ambient temperature as well as on the electrode material. The positive shift in the value of E_{corr} for both samples with temperature rise indicates more stable passive films on their surfaces. Fig. 9(a, b) reveals that both corrosion and critical current densities are lowered by an increase in temperature, indicating inhibition in the rate of dissolution process for the corroding-passivating surface oxide film. At room temperature and above, the values of the two current densities (i_{corr} and i_{crit}) seem to be constant, especially for pure Ti sample, whereas they rise sharply as the temperature is lowered more than the room value. The enhanced passive film formation for the two materials upon raising temperature is consistent with a decrease in the aggressive Br^- ion concentration in the interface region as a result of a decrease in the extent of anion adsorption at high temperature [51]. Also, raising solution temperature improves the passive properties of the surface films by decreasing the concentration of anion vacancies present on titanium oxide film.

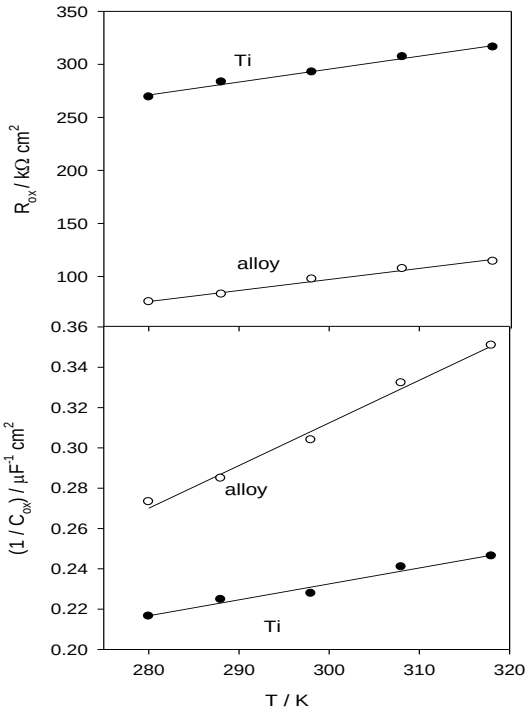

Figure 8. Dependence of R_{ox} and $1/C_{ox}$ for titanium and Ti-6Al-4V alloy on the ambient temperature of 1.0 M HBr solution.

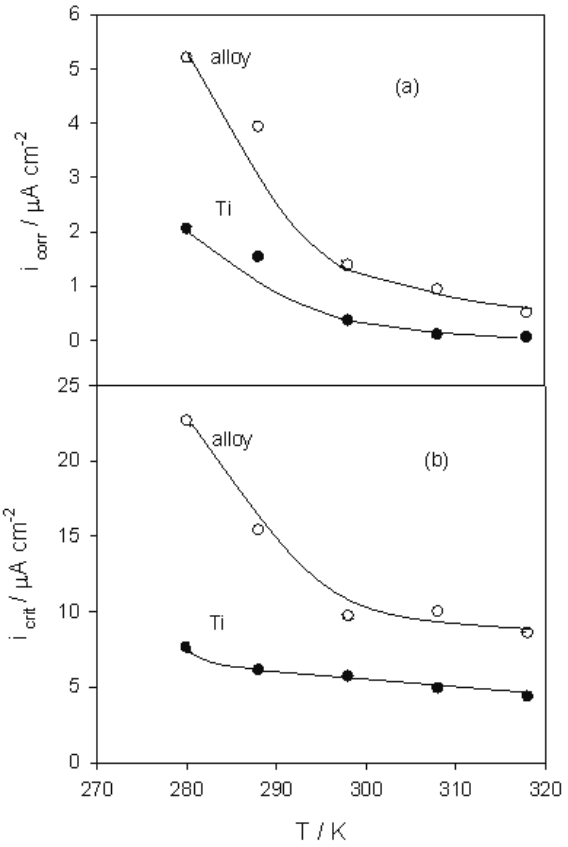

Figure 9. Variation of: (a) the corrosion (i_{corr}) and (b) the critical (i_{crit}) current densities with temperature for Ti and Ti-6Al-4V alloy in 1.0 M HBr solution.

Table 5. Electrochemical corrosion parameters of Ti and Ti-6Al-4V alloy in 1.0 M HBr solution at various temperatures.

Electrode	T / K	E_{corr} /	i_{corr} /	η_a /	η_c /	i_{crit} /
		$mV_{Ag/AgCl}$	□□μA cm^{-2}	mv/decade	mv/decade	μA cm^{-2}
Ti	280	265	2.05	264	-434	7.6
	288	295	1.53	227	-457	6.1
	298	320	0.36	211	-413	5.7
	308	305	0.10	252	-357	4.9
	318	461	0.05	306	-419	4.4
Ti-6Al-4V	280	-180	5.20	338	-230	22.7
	288	-170	3.93	174	-347	15.4
	298	260	1.38	91.9	-97.5	9.7
	308	350	0.93	68	-87.1	10.0
	318	480	0.50	46	-72.8	8.6

These anion vacancies are generated by the presence of lower titanium oxidation states [52]. On the other hand, the high current density obtained for Ti-6Al-4V alloy compared to Ti metal might be due to the effect of alloying elements (Al and V) in the passive film of the former. Aluminium and vanadium likely enter the lattice of the passive film making it less protective and so decrease the corrosion resistance and stability of the sample more than in case for the pure base metal. The inferior corrosion performance of Ti-6Al-V relative to Ti has been reported recently by the same author [19,28].

As far as the results of the three used electrochemical techniques are concerned, it may be assumed that ingress of aggressive Br^- anion into the oxide film via adsorption mechanism, leads to nucleation of corrosion pits at the active inclusion sites mainly due to formation of titanium tetrabromide ($TiBr_4$) or oxybromide ($TiOBr_2$). These pit nuclei do not propagate, but simply repassivate immediately by re-growth of the oxide film via the hydrolysis of the covalent tetrahalide to give TiO^{++} or TiO_2 depending on the bulk pH and the ambient conditions [43]. Raising solution temperature activates also the simultaneous hydrolysis process and consequently sustains the re-passivation kinetics.

4. CONCLUSIONS

1. The influence of low and highly concentrated HBr solutions (0.01 M–8.0 M) on the corrosion and passivation behavior of titanium and Ti-6Al-4V alloy was investigated by OCP, EIS and potentiodynamic polarization tests.

2. Over the whole concentration domain the OCP increases positively with time, indicating self-passivation for both samples, where there is an optimum HBr concentration at which the thickening rate for the two layers comprising the formed oxide film is maximum.

3. For Ti metal, EIS results showed that the relative film thickness ($1/C_{ox}$) and its resistance (R_{ox}) exhibit fast increase up to 0.5 M followed by a gradual decrease. However, in case of Ti-6Al-4V alloy the general trend of the above two parameters is to decrease continuously as HBr concentration is increased with no sign for a threshold value.

4. The two corrosion parameters i_{corr} and i_{crit} derived from the polarization curves, both exhibit a reverse trend in corroborating with the above behavior.

5. In a moderate HBr concentration (1.0 M), temperature can act as a catalyst for easier passivation of the two tested samples, leading to decrease their corrosion rates. Over the studied temperature range (280-318 K), the increase in the thickening rate of the spontaneously formed oxide layers follows Arrhenius behavior and the calculated apparent activation energies for the process confirm well that Ti has a stronger propensity to form passive film in HBr solution more than its Ti-6Al-4V alloy.

References

1. P. Kovacs, J. A. Davidson, in: S. A. Brown, J. E. Lemons (Eds.), *Medical Applications of Titanium and its Alloys: The Materials and Biological Issues*, ASTM, STP 1272 (1996) pp. 163-178.
2. C. Sittig, M. Textor, N.D. Spencer, M. Wieland, P.-H. Vallotton, *J. Mater. Sci.: Mater. Med.* 10 (1999) 35-46.
3. C. Fonseca, M.A. Barbosa, *Corros. Sci.*, 43 (2001) 547-559.
4. S.L. de Assis, S. Wolynec, I. Costa, *Electrochim. Acta*, 51 (2006) 1815-1819.
5. D.J. Blackwood, R. Greef, L.M. Peter, *Electrochim. Acta*, 34 (1989) 875-880.
6. T. hurlen, S. Hornkjol, *Electrochim. Acta*, 36 (1990) 189-195.
7. J. R. Birch, T. D. Burleigh, *Corrosion*, 56 (2000) 1233-1241.
8. C.E.B. Marino, E.M. de Oliveira, R.C. Rocha-Filho, S.R. Biaggio, *Corros. Sci*., 43 (2001) 1465-1476.
9. J.M. Abd El-Kader, F.M. Abd El-Wahab, H.A. El-Shayeb, M.G.A. Khedr, *Br. Corros. J*., 16 (1981) 111-114
10. A.G. Gad- Allah, H.A. Abd El-Rahman, *Corrosion*, 43 (1987) 698-702.
11. R.D. Armstrong, J.A. Harrison, H.R. Thirsk, R. Whitfield, *J. Electrochem. Soc*., 117 (1970) 1003-1006.
12. Lj. D. Arsov, *Electrochim. Acta*, 30 (1985) 1645-1657.
13. Lj.D. Arsov, *Electrochim. Acta*, 27 (1982) 663-672.
14. W. Wilhelmsen, T. Hurlen, *Electrochim. Acta*, 32 (1987) 85-89.
15. T. Ohtsuka, M. Massuda, N. Sato, *J. Electrochem. Soc*., 132 (1985) 787-792.
16. J. Joseph, A. Gagnaire, *Thin Solid Films*, 103 (1983) 257-265.
17. Her-Hsiung Huang, *Electrochim. Acta*, 47 (2002) 2311-2318.
18. N.D. Tomashov, G.P. Chernova, Yu.S. Ruscol, G.A. Ayuyan, *Electrochim. Acta*, 19, (1974) 159-172.
19. F. El-Taib Heakal, A.A. Ghoneim, A.S. Mogoda, Kh.M. Awad, *Corros. Sci.*, 53 (2011) 2728-2737.
20. B. Grosgogeat, M. Boinet, F. Dalard, M. Lissac, *Bio. Med. Mater. Eng*., 14(2004) 323-331.
21. M.S. El-Basiouny, A.G. Gad Allah, *Annali di chimica*, 71 (1981) 391-399.
22. M.M. Hefny, A.G. Gad Allah, S.A. Salih, M.S. El-Basiouny, *Corrosion*, 40 (1984) 245-249.

23. G.T. Burstein, R.M. Souto, *Electrochim. Acta*,40 (1995) 1881-1888.
24. G.O. Tatarchenko, Zh.G. Makarova, A.N. Kuzyukov, *Mater. Sci*., 38 (2002) 430-435.
25. V.R. Savochkin, I.N. Nagai, A.M. Sukhotin, *Zashchita Metallov*, 7 (1971) 297-298.
26. N.D. Tomashov, I.N. Nagai, D.K. Seledtsov, V.M. Kochergina, V.I. Kazarin, B.A Goncharenko, V.S. Mikkeev, *Zashchita Metallov*, 19 (1983) 205-211.
27. J.A. Petit, B. Kondro, F. Dabosi, *Corrosion*, 36 (1980) 145-151.
28. A.A. Ghoneim, F. El-Taib Heakal, A.S. Mogoda, Kh.M. Awad, *Surf. Interface Anal*., 42 (2010) 1695-1701.
29. N.T.C. Oliveira, A.C. Guastaldi, *Corros. Sci*., 50 (2008) 938-945.
30. A.G. Gad Allah, A.M. Bekheet, S.S. El-Egamy and M.S. El-Basiouny, *Bull. Electrochem*., 7 (1991) 397-401.
31. L. Young, Anodic Oxide Films, Academic Press, London (1961).
32. D.D. Macdonald, *Pure Appl. Chem*., 71 (1999) 951-986.
33. M.F. Lopez, M.L. Escudero, *Electrochim. Acta*, 43 (1998) 671-678.
34. F. El-Taib Heakal, S. Haruyama, *Corros. Sci*., 20 (1980) 887-898.
35. J.R. Macdonald, in Impedance Spectroscopy Emphasizing Solid Materials and Systems, John Wiley & Sons, New York (1987).
36. F. El-Taib Heakal, A.A. Ghoneim and A. Fekry, *J. Appl. Electrochem*. 37 (2007) 405-413.
37. F. El-Taib Heakal, A.S. Mogoda, A.A. Mazhar, M.S. El-Basiouny, *Corros. Sci.*, 27 (1987) 453-4462.
38. K. Juttner, *Electrochim. Acta*, 35 (1990) 1501-1508.
39. F. El-Taib Heakal, M. Ameer, A. El-Aziz, A. Fekry, *Mat.-wiss. u. werkstofftech*. 35 (2004) 407-412.
40. R. Schutz, An Overview of Beta Titanium Alloy Environmental Behaviour, in Beta Titanium Alloy in the 1990's, D. Eylon, R. Boyer, D. Koss, (Eds): *The Mineral, Metals & Materials Society* (1993) pp. 75-91.
41. P. Zoltowski, *J. Electroanal. Chem*., 375 (1974) 45-57.
42. N. Casillas, S. Charlebois, W. H. Smyrl and H. S. White, *J. Electrochem. Soc*., 141 (1994) 636-642.
43. T. R. Beck, *J. Electrochem. Soc*., 120 (1973) 1310-1316.
44. F. El-Taib Heakal, A. Fekry, A. Ghoneim, *Corros. Sci*., 50 (2008) 1618-1626.
45. F. El-Taib Heakal, A. Fekry, M.Z. Fatayerji, *J. Appl. Electrochem*., 39 (2009) 583-591.
46. H. H. Uhlig, Corrosion and Corrosion Control, John Wiley and Sons, New York (1971) p. 75.
47. V. Zwilling, M. Aucouturier, E. Darque-Ceretti, *Electrochim. Acta*, 45 (1999) 921- 929.
48. T. Shibata, Y.-C. Zhu, *Corros. Sci*. 36 (1994) 153-163.
49. D.J. Blackwood, L.M. Peter, *Electrochim. Acta*, 34 (1989)1505-1511.
50. T. Shibata, Y.-C. Zhu, *Corros. Sci*., 37 (1995) 133-144.
51. A.Despic and V. Parkhutik in Modern Aspects of Electrochemistry, (Eds.): J.O'M. Bockris, R.E. White, B.E. Conway, Vol. 20, Plenum Press, New York (1989) p. 440.
52. S. Tamilselvi, V. Raman, N. Rajendran, *Electrochim. Acta*, 52 (2006) 839-846.